Applied Surface Science 736 (2026) 166710

Contents lists available at ScienceDirect

Applied Surface Science

journal homepage: www.elsevier.com/locate/apsusc

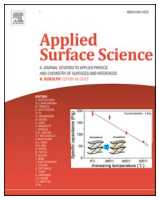

Full Length Article

Breaking the pattern: structure and fundamental properties of bismuth and tellurium adlayers on platinum basal surfaces

Andrey A. Koverga [a,*], Ana María Gómez-Marín [b], Elizabeth Flórez [c], Edson A. Ticianelli [a]

[a] Instituto de Química de São Carlos, Universidade de São Paulo, São Carlos, SP, Brazil
[b] Instituto Tecnológico de Aeronáutica, São Jose dos Campos, SP, Brazil
[c] Grupo de Investigación Mat&mpac, Facultad de Ciencias Básicas, Universidad de Medellín, Medellín, Colombia

ARTICLE INFO

Keywords:
DFT
Pt
Catalysis
Adatoms
Coverage

ABSTRACT

In this computational study the explicit interaction of Bi and Te with (111), (110), and (100) platinum surfaces was investigated, focusing on structural and electronic characteristics of the studied systems as a function of the adsorbate coverage. For Bi/Pt systems, good agreement was found between calculated results and previously published data. At all coverages adsorbed Bi or Te atoms interact repulsively. At coverages close to half a monolayer the structure of the adlayers on more open Pt(110) and (100) surfaces is defined by the geometry of the substrate, while on densely packed Pt(111) the regular pattern breaks and adsorbed Bi or Te layers become more disordered, as experimentally reported for Bi. Additionally, whereas the downshift on the *d*-band centre of Pt atoms in contact to the adatoms weakens the Pt-Bi(Te) bond, the depolarization of the adlayer contributes to the stabilization of the adatom-adatom interaction within the adlayer. Obtained results evidence that Bi and Te adlayers supported on Pt cannot be treated as a mere combination of their parts and, instead, must be considered as unique materials with properties different from their parent systems.

1. Introduction

Our civilization is constantly growing in complexity, relying on an increasing number of (electro)chemical processes across numerous industrial branches of various scales. Developing efficient catalysts for these processes is essential for advancing technology and achieving sustainable economic growth, urging the search for materials with catalytic properties finely tuned to meet the requirements of specific target reactions. One promising approach is the selective decoration of metallic and non-metallic surfaces with atoms of foreign elements, which is known to affect fundamental and catalytic properties of the initial materials [1–3].

Typically, the effects of the adsorbed foreign atoms are divided into three categories: third-body, bifunctional, and electronic effects. Third-body effects occur when the adsorbed atom, or adatom, blocks surface sites prone to poisoning or formation of undesirable products, steering the reaction along the desired path. Bifunctional mechanism describes the situation when the adatom directly interacts with reactants and reaction intermediates, providing alternative adsorption sites, thus, affecting reaction rates or mechanisms or even forming new products. Finally, electronic effects occur when the foreign species modify fundamental properties of the substrate, directly related to its (electro) catalytic activity, such as its work function [4], charge distribution [5], and electronic structure of the surface atoms [6].

Unfortunately, for any given adsorbate–substrate system the effect of the adatom can fall in either of these categories or be a combination of thereof, which is why experimentally it is difficult to precisely identify how exactly the foreign species affect (electro)catalytic properties of resulting systems [7]. Also, the adatom–substrate interaction depends on the nature of the interacting adsorbate and host surface, complicating even further the analysis.

Since platinum is the best-known catalyst for several (electro)catalytic processes important for energy conversion and storage, it is historically one of the most studied metals. Because of the enormous amount of information available on Pt-based systems, selective decoration of platinum surfaces not only presents a viable strategy for designing new (electro)catalytically active materials, but also could serve as a valuable case study for a better understanding of catalytic systems. It may enable efficient identification of active surface sites, and/or the chemical composition of active centres allowing to shed light on complex correlations between reactivity of the catalyst and its surface structure and composition [8–10].

* Corresponding author.
E-mail address: akoverga@unal.edu.co (A.A. Koverga).

https://doi.org/10.1016/j.apsusc.2026.166710
Received 8 September 2025; Received in revised form 22 March 2026; Accepted 23 March 2026
Available online 27 March 2026

In this regard, the interaction of platinum with several adatom species in the context of (electro)catalytic properties of resulting composite systems has been studied both experimentally [2,8–26] and theoretically [27–29]. While the impact of different foreign atoms on the (electro)catalytic properties of platinum has been analysed, most often it was explained in terms of third-body effect, evidently overlooking more intricate details of the adatom-substrate interaction. Thus, despite significant research efforts, the current understanding of the adatom effect on the atomistic level largely remains unclear and requires further investigation. In respect to this, although limited, few studies have offered some insight into the adatom-induced changes in the fundamental properties of platinum surfaces upon adatom adsorption [5,18,25,29,], discussing in detail changes in the work function and electronic structure of the substrates. These works have also demonstrated that accounting for adatom's coverage is extremely important for a more accurate description of these catalysts, bringing the theoretical models closer to realistic systems [18,25].

Decorating platinum surfaces with Bi and Te is known to modify the catalytic activity of platinum toward reactions significant to energy conversion [8–17,21–24,26]. There are plenty of experimental studies, mainly under the electrochemical environment, evidencing the importance of these systems in modifying the electrocatalytic activity of Pt basal planes, and polycrystalline Pt toward key reactions of interest [1–3,5,8–17,19,23,26], such as the oxidation of many organic molecules (formic acid, methanol, ethanol, among others). In many cases, while large reactivity enhancements have been reported on some basal planes, no effect, or even inhibition has been found on the other surfaces. The reasons behind these experimental facts mostly remain unknown, although some simple models have been reported.

An earlier theoretical study elucidated the impact of a single Bi or Te atom on fundamental properties of Pt(111), Pt(110), and Pt(100) surfaces, and made a link between the adatom effect on practically observed changes in catalytic activity of platinum toward various electrochemical processes [29]. It clearly showed the important role of the theoretical approach for identifying the electronic effects of adatoms and their implications for the catalytic properties of platinum were discussed in detail. However, models used in the mentioned study did not include the analysis of the complex adatom–substrate, and adatom–adatom interactions, emerging when several adatoms are present simultaneously on the surface, and, potentially, contributing to the shift of the catalytic activity of the composite system.

Therefore, a density functional theory study of platinum surfaces, modified with submonolayer coverages of bismuth and tellurium, becomes essential as a first step toward a systematic understanding of the reasons behind reported increases on the electrocatalytic activity. This study could shed light on the impact of Bi and Te adatoms on the evolution of fundamental properties of platinum with increasing adatoms' coverage. Moreover, because of the level of generality and transferability of these calculations, results can potentially be expanded, as a preliminary assessment, toward other important similar adatom-modified Pt electrocatalytic systems, such as Sn-, Ge-, As- and Sb-Pt. This information is crucial for establishing new and efficient strategies for the design of novel electrocatalytic materials.

It is important to highlight, though, that calculations performed in vacuum cannot be immediately tied to the experimentally observed Bi- or Te-induced changes in catalytic activity of platinum toward specific electrochemical processes due to the complexity of the practical catalytic systems and reactions. In particular, beside electronic properties of the electrode, factors such as the solvent, spectator ions, electrode potential, interfacial electric fields, and specific adsorption of reaction intermediates also play an important role in electrocatalysis. Consequently, the adatom-induced changes in the fundamental properties of platinum surfaces alone cannot provide quantitative predictions of catalytic activity under operating electrochemical conditions.

However, the intrinsic electronic properties of clean and modified metal surfaces that have a direct impact on interaction of reactants and reaction intermediates with the surface, such as work function and *d*-band centre, are largely defined by the electronic configuration of the metal and local coordination. At the same time, it has been found that the direct interaction of water with transition metal surfaces does not dramatically affect local density of states of the metal, entailing only modest changes in adsorption energies of other adsorbates [30]. Thus, the qualitative trends discussed in the present study will be relevant for understanding changes in catalytic properties of platinum decorated with bismuth or tellurium.

The present work, therefore, aims to explore changes in the charge distribution, the work function, and the electronic structure of model Pt (111), Pt(110), and Pt(100) surfaces, caused by adsorption of bismuth and tellurium at coverages up to half a monolayer. In realistic systems under electrochemical conditions complex structural phenomena can potentially emerge, including surface reconstruction [31], alloying, clustering, or potential-dependent ordering of overlayers [31–36]. However, as the first step toward understanding the Bi- and Te-modified Pt systems, this study did not explicitly consider these effects to systematically investigate the effect of the adatom coverage, adatom-substrate, and adatom-adatom interactions. The trends for the fundamental properties of platinum surfaces were analysed as a function of coverage of the adatoms and their nature. Additionally, the geometrical structure and stability of the adlayers, and factors impacting their formation and growth were also discussed in detail.

2. Computational details

In the present study periodic spin-polarized density functional theory (DFT) calculations were performed using Vienna *ab initio* simulation package (VASP) [37–40]. The exchange–correlation effects were accounted within the generalized gradient approximation by Perdew, Burke and Ernezerhof [41]. This is a common choice for studying transition metal-based systems where the metal is either substrate or adsorbing species, yielding accurate description of their fundamental characteristics [18,25,42–44]. The core electrons were represented by the Projector Augmented Wave core potentials [45] as implemented by Kresse and Joubert [46]. An energy cut-off of 415 eV was chosen for a plane-wave basis set to assure convergence of the calculations.

For the geometry optimisation calculations, the reciprocal space for all considered surfaces was described within Monkhorst-Pack approach [47] with a $5 \times 5 \times 1$ k-points sampling. A denser $10 \times 10 \times 1$ grid was used for Density of States calculations. In all cases the Fermi level was smeared using first order Methfessel-Paxton approach [48] with 0.2 eV Gaussian width of smearing. All necessary calculations for isolated atoms were carried out in $8 \times 8 \times 8$ Å cubic cell using similar parameters as described above but with single Γ-point sampling.

Model platinum (111), (110), and (100) surfaces were created from an optimized platinum bulk structure with the calculated equilibrium lattice parameter, *a*, of 3.97 Å, in a good agreement with the values available throughout the literature [49,50]. The range of coverages between 0.06 ML and 0.50 ML on the Pt (1 1 1) surface was studied using a (4×4) supercell, containing 16 atoms in its topmost layer, while a $\left(2\sqrt{3} \times 2\sqrt{3}\right)$ supercell with four adatoms was employed to model the 0.33 ML adatom coverage. The (1 1 0) and (1 0 0) surfaces were modelled using (3×3) supercell with 18 surface atoms. All supercells comprised four atomic layers, with the two bottom layers frozen in the bulk-like geometry. The two upper layers were allowed to relax simultaneously together with the adsorbed atoms (adatoms) present on the surface during structural optimization.

To prevent possible interactions between supercell images repeating in the direction, perpendicular to the surface, a vacuum region of 18 Å was introduced to all systems and dipole corrections were applied. Structural optimization was complete when the variation in the total forces was smaller than 0.01 eV/Å at the current and previous step.

This study focused on the systems with Bi and Te adlayers on Pt(*hkl*)

surfaces, denoted here as Bi/Pt(*hkl*) and Te/Pt(*hkl*), respectively. Single Bi and Te atom adsorption was considered on surface sites summarized in Fig. 1. Minimal coverage on Pt(111), thus, was 0.06 ML, while on Pt (110) and Pt(100) –0.05 ML.

By selecting the systems with the most negative adsorption energy the fcc site on Pt(111) and four-fold hollow sites on Pt(110) and (100) were identified as preferable for both adatoms. Following this, an analysis was conducted on whether at non-minimal coverages the newly added atoms would adsorb next to adatoms already present on the surface, or rather occupy an adsorption site located further away from them. For this, two Bi or Te atoms were placed on the neighbouring stable sites on each surface (fcc sites on Pt(111), and four-fold hollow – on Pt(110) and (100)) and on the sites that were separated by not less than 5 Å, as shown in Fig. S1.

After relaxation, it was evident that on Pt(111) simultaneous adsorption of two atoms on the neighbouring sites is energetically less favourable than on the separated sites by 0.30 eV and 0.45 eV for Bi and Te, respectively, due to the repulsive Bi-Bi and Te-Te interaction emerging when two adatoms are adsorbed next to each other. Importantly, this comparison also indicates stronger repulsive Te–Te interaction compared to the Bi–Bi one.

The distance between neighbouring four-fold hollow sites on the Pt (110) and (100) surfaces is larger, compared to the that between fcc sites on more densely packed Pt(111). As a result, the repulsive Bi-Bi and Te-Te interactions on these surfaces are not as strong as on Pt(111). On Pt (110) bismuth atoms adsorbed at a distance from each other were 0.16 eV more stable than those adsorbed on the neighbouring sites, and for Te this difference was 0.23 eV. The Pt(100) surface represents an intermediate case between Pt(111) and Pt(110), since separation of the adatoms led to the stabilization of 0.19 eV and 0.27 eV for bismuth and tellurium, respectively.

The interaction of Pt surfaces with growing overlayers of Bi and Te was studied by placing the adatoms one by one onto the stable adsorption sites separated from each other on the model surfaces, when possible, until half a monolayer coverage was reached. This approach enabled calculations of experimentally reported $p(2 \times 2)$, and $(\sqrt{3} \times \sqrt{3})R30^o$ patterns formed on Pt(111) at 0.25, and 0.33 ML, resp., for adsorption of both Bi [32,33,51], and Te [35,36], and the $c(2 \times 2)$ structure for adsorption of Bi on Pt(100) at 0.5 ML [34,52], under both UHV and electrochemical conditions.

The differential adsorption energy for each n^{th} adatom was calculated as:

$$E_{ads,n} = E_{nBi(Te)/Pt} - E_{Bi(Te),g} - E_{(n-1)Bi(Te)/Pt} \quad (1)$$

where $E_{nBi(Te)/Pt}$ and $E_{(n-1)Bi(Te)/Pt}$ are total energies of systems comprising n and n-1 Bi or Te atoms on Pt surface, respectively and $E_{Bi(Te),g}$ – total energy of the isolated Bi or Te atom in vacuum. This approach to calculating adsorption energy provides insight into how adding an atom to the adlayer affects its stability.

The degree of strain allows to estimate how"compressed" or"stretched" is the adlayer due to the presence of Pt substrate in respect to corresponding stable bulk structure (rhombohedral for Bi and trigonal – for Te) and it was calculated as indicated earlier in the literature [53,54]:

$$S = \frac{d_{Bi(Te)-Bi(Te),adl} - d_{Bi(Te)-Bi(Te),bulk}}{d_{Bi(Te)-Bi(Te),bulk}} \times 100\% \quad (2)$$

where $dBi(Te) - Bi(Te),adl$ and $dBi(Te) - Bi(Te),bulk$ are average distances between the atoms in adsorbed adlayer and in stable bulk structures, respectively. From this formalism, positive values of S would correspond to the adlayer stretching, negative – to its compression, relative to the bulk Bi(Te).

Work function, Φ, for pristine and adatom-modified platinum surfaces was calculated as difference of electrostatic potential in vacuum, V_∞, and the Fermi level of the surface, E_F:

$$\Phi = V_\infty - E_F \quad (3)$$

Since bismuth, tellurium and platinum are heavy elements, the impact of spin–orbit coupling (SOC) effect on adsorption energies and work functions was evaluated as well. Specifically, trends in adsorption energies and work functions obtained with and without including the SOC effect into calculations were compared.

Adatom-induced charge redistribution was analysed by employing four different calculations. A Density Derived Electrostatic and Chemical (DDEC6) partitioning scheme [55,56], with net charges on atoms calculated with Chargemol [56], the Bader charge analysis [57], as implemented in VASP by Henkelman, Arnaldsson and Jonsson [58]. In the latter case, the total net charge for platinum, bismuth and tellurium atoms were calculated as a difference between the number of valence electrons in the corresponding isolated atom, Z_A, and obtained Bader charge value, $q_{A,\ Bader}$ for the same atom in the adsorbate–substrate system:

$$QA = ZA - q_{A,Bader} \quad (4)$$

A third approach for approximating the maximum adatom-induced charge, Q_{max}^{CDD}, was by integrating along z-axis, perpendicular to the surface plane, curves of the charge density differences (CDD) calculated as

$$\Delta\rho = \rho_{Pt+Bi(Te)} - \rho_{Pt} - \rho_{Bi(Te)} \quad (5)$$

where $\rho_{Pt\ +\ Bi(Te)}$ is the charge distribution in the system with an adatom on a Pt surface (the whole interacting system), and ρ_{Pt} and $\rho_{Bi(Te)}$ are the charge distributions for the pristine surface, and for the adatom species in the gas phase (the isolated, non-interacting components of the whole system), but with the exact same geometry as in the composite, interacting system [29], respectively.

Finally, the fourth method for estimating the adatoms-charge was by calculating the equivalent charge of a dipole with a magnitude similar to the change in the work function upon adatoms's adsorption, and at separation equal to the distance between the surface and the adatom. The calculation of the surface dipole from the change in the work function was made through the Helmholtz equation [29].

The d-band centre for platinum atoms was calculated as first moment of the projected d-band density of states, $\rho(x)$, in respect to the Fermi

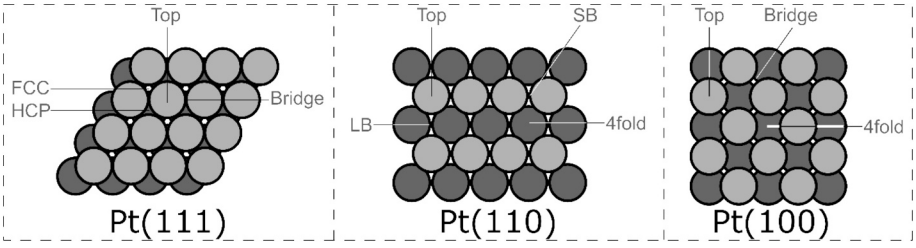

Fig. 1. Adsorption sites considered on the Pt(111), (110) and (100) surfaces. For Pt(110) short bridge (SB) and long bridge(LB) sites are illustrated. Surface platinum atoms are represented by light-grey spheres, while dark-grey spheres indicate Pt atoms in the sublayers.

level [59]:

$$\varepsilon_d = \frac{\int_{-\infty}^{\infty} x\rho(x)dx}{\int_{-\infty}^{\infty} \rho(x)dx} \quad (6)$$

3. Results and discussion

3.1. Interaction of single Bi or Te atom with model platinum surfaces

The detailed analysis of a single Bi and Te atom interaction with Pt surfaces can be found in the earlier study [29], while here certain crucial characteristics of Bi/Pt and Te/Pt systems are summarized in Table 1. Both adatom species are very stable on the considered surfaces, in agreement with the experimental results available on Bi [32,33,51] and Te [35,36] interaction with Pt(111) and Bi on Pt(100) [34,52]. It must be noted here that the adsorption energy values obtained for Bi without accounting for SOC effect are closer to experimental ones than those calculated including SOC. Specifically, E_{ads} for Bi on Pt(111) calculated without SOC was −3.31 eV, closer to the experimental value of −3.52 eV [51] than −3.84 eV calculated accounting for SOC. Similarly, for Bi adsorbed on Pt(100) the adsorption energy without SOC was −3.87 eV, while accounting for SOC resulted in much more negative value of −4.40 eV, significantly further from the experimental value of −3.95 eV [52].

The electron localization function (ELF) analysis revealed that both adatom species interact with platinum in a similar fashion, forming a mixed covalent-metallic Bi–Pt and Te–Pt bonds [29]. Based on calculated total net charges, within the Density Derived Electrostatic and Chemical (DDEC6), Bader partitioning schemes and by approximating the maximum adatom-induced charge, an adatom → surface charge transfer is seen, following differences on electronegativity between Pt and adsorbed species in the Pauling scale ($\xi_{Pt} = 2.2$, $\xi_{Bi} = 1.9$, and $\xi_{Te} = 2.1$). In agreement, adatom → surface charge transfer is also found in all cases by the integration of curves of the charge density difference (CDD) for each system, and these results are resumed in Fig. S2.

For the Bi/Pt ad Te/Pt systems the Q_{max}^{CDD} scheme as well as both DDEC6 and Bader approaches agree on the charge transfer direction, similarly to reported results obtained with either the Hiershfield or Mulliken formalism [19]. Importantly, maximum charge transfer estimated from Δρ can be seen as just another "partitioning" scheme to estimate the adatom's charge. Hence, the uncertainly regarding the selection of the position of z-plane that separates positive and negative excess charge densities at the interface, inherent to all approaches to dividing the total electron density into atomic contributions [60], is also characteristic to this method as well.

While each method predicted different total net charge values for the adatoms, neither of the approaches reflected completely the adatom-induced changes in the work function, which are not uniform and more sensitive to the surface orientation [61]. Thus, all discussed partitioning schemes offer a valid first estimate of the trends in charge transfer upon adatom–substrate interaction at different coverages. In the present study the DDEC6 scheme was used since it better handles delocalized electrons than the Bader scheme, which is crucial for metallic systems [56].

Regarding the adatom-induced changes in electronic structure of platinum atoms, the *d*-band centre, ε_d, values become more negative upon adsorption of either Bi or Te single atom, i.e. a noticeable shift of the average *d*-band centre further away from the Fermi level is seen for the surface atoms directly in contact with the adsorbed species, in agreement with experimentally observed enhancement of oxygen reduction reaction on Te-modified platinum surfaces [26]. This shift is manly defined by the ligand effect [62] caused by the adsorbate–substrate interaction, specifically, through *s* and *p* outer shell electrons of Bi and Te and 5*d* electrons of Pt [29].

3.2. Interaction of Bi or Te with model platinum surfaces at increasing adatom coverage

The coverage-dependent interaction of Bi and Te adlayers with model platinum surfaces was studied in the range of $\Theta_{Bi(Te)}$ from 0.06 ML to 0.50 ML on Pt(111) and from 0.05 ML to 0.50 ML – for Pt(110) and (100). Through studied coverages both Bi and Te tend to interact repulsively in the adlayer, occupying the available surface sites as far as possible from the adatoms already adsorbed on the substrate. Importantly, at coverages higher than 0.25 ML several alternative adatom arrangements become possible on all considered surfaces, including different adatom in-plane distribution and aggregation. Thus, for coverages higher than 0.25 ML several alternative 2D structures have been tested. In this work, reported structures were built up by selecting the lowest-energy configurations after addition of the "*new*" adatom at increasing coverages. Thus, although experimentally reported $p(2 \times 2)$, and $\left(\sqrt{3} \times \sqrt{3}\right)R30^o$ superstructures at 0.25, and 0.33 ML for both Bi/Pt(111) [32,33,51], and Te/Pt(111) [35,36], and the $c(2 \times 2)$ pattern for Bi/Pt(100) at 0.5 ML [34,52], under both UHV and electrochemical conditions, were calculated, as highlighted above, other superstructures at different coverages may have been not included [32–36,51,52].

On Pt(111) at coverages up to 0.25 ML, corresponding to 4 adatoms on the surface simultaneously, Bi and Te are able to adsorb maintaining maximum separation and minimizing the repulsive adatom-adatom interaction. As the result, a $p(2 \times 2)$ structure at 0.25 ML forms on Pt (111) where distances between the adatoms are mainly defined by the distances between the non-neighbouring fcc surface sites. The geometry of the adlayer has a structure resembling that of the substrate with the distance between the adsorbed atoms ~ 5.6 Å in both Bi/Pt(111) and Te/Pt(111) systems. Thus, the degree of strain for Bi and Te adlayers at this coverage were +67% and +76%. This corresponds to the overlayers being stretched, comparing to the corresponding bulk structures with interatomic distances of 3.34 Å and 3.19 Å for Bi and Te, respectively.

With the coverage growing from 0.25 ML to 0.50 ML the surface

Table 1
Preferable adsorption site, calculated adsorption energy (E_{ads}), distance between the adatom and the surface ($d_{Bi(Te)–Pt}$), Pt–Pt distances in the proximity of the adatom ($d_{Pt–Pt}$), total net charge values for the adatoms calculated using the DDEC6 scheme($Q_{B(Te)}^{DDEC6}$), Bader approach ($Q_{B(Te)}^{Bader}$), and Q_{max}^{CDD} approach for single Bi and Te adsorbed on the model Pt surfaces. Adatom-induced changes in the work function (ΔΦ) and d-band centre positions for Pt atoms are indicated as well.

System	Site	E_{ads} (eV)	$d_{Bi(Te)–Pt}$ (Å)	$d_{Pt–Pt}$ (Å)[a]	$Q_{B(Te)}^{DDEC6}(e)$[b]	$Q_{B(Te)}^{Bader}$(e)[b]	Q_{max}^{CDD}(e)[c]	$\Delta\varepsilon_d$ (eV)[d]
Bi/Pt(111)	fcc	−3.31	2.11	2.95	+0.45	+0.73	+0.26	−0.32
Te/Pt(111)	fcc	−3.82	1.92	3.07	+0.27	+0.51	+0.17	−0.41
Bi/Pt(110)	4fold	−3.99	1.49	2.86 / 3.88	+0.39	+0.72	+0.15	−0.13
Te/Pt(110)	4fold	−4.38	1.29	2.89 / 3.86	+0.26	+0.52	+0.10	−0.16
Bi/Pt(100)	4fold	−3.87	1.91	2.91	+0.42	+0.69	+0.19	−0.19
Te/Pt(100)	4fold	−4.44	1.72	2.94	+0.28	+0.51	+0.14	−0.24

[a] For Bi(Te)/Pt(110) surfaces the distances between Pt atoms in the short-bridge and long-bridge adsorption sites are indicated.
[b] Positive values correspond to charge loss.
[c] The maximum adatom-induced charge, calculated by integrating the charge density difference curves along z-axis, perpendicular to the surface plane.
[d] Calculated values for ε_d of Pt(111), Pt(110) and Pt(100) were −2.59 eV, −2.32 eV and −2.51 eV, resp.

becomes more "crowded" and adatoms are not able to maintain the maximum separation. The repulsive interaction leads to the breaking of initially surface-defined adlayer pattern. A significant distortion of the hexagonal organization of the adlayers on Pt(111) is seen by $\Theta_{Bi(Te)} >$ 0.33 ML and adatoms shift from their stable fcc sites, occupied at low coverages, to other (initially) less stable locations. In agreement with available experimental data [51], resulting structures do not follow a hexagonal structure anymore and become less stretched compared to the adlayers at lower coverages, as evidenced by the degrees of strain of +8% and +20% calculated for Bi and Te at half a monolayer coverage.

On Pt(110) and (100) surfaces, that are less densely packed than Pt (111), the tendency of the adatoms to adsorb at a distance from each other combined with the larger separation of the stable adsorption sites led to a significant stretching of the Bi and Te adlayers at lower coverages up to $\Theta_{Bi(Te)} = 0.22$ ML, corresponding to four-atoms adlayers. The calculated degrees of strain for the adlayers on Pt(110) at this coverage were +104% and +114% for Bi and Te, resp., indicating extreme overlayer stretching in respect to the corresponding bulk structures. On Pt(100) the stretching of the adlayers at $\Theta_{Bi(Te)} = 0.22$ ML was smaller, corresponding to 64% for Bi and 71% – for Te adlayers compared to the their bulk geometries.

The adlayers get somewhat less strained with the growing coverage: at $\Theta_{Bi(Te)} = 0.50$ ML the average adatom distances in the Bi and Te structures on Pt(110) are 44% and 51% longer compared to the distances in the respective bulk structures. On Pt(100) the estimated degrees of strain were +19% for Bi and +24% for Te – smaller than on Pt (110) because of shorter distance between the stable adsorption sites. As in the Bi(Te)/Pt(111) systems the adlayers organize in the patterns defined by that of the substrate, and on Pt(100) both adatoms form a $c(2 \times 2)$ pattern at 0.5 ML. However, unlike it occurred on Pt(111), no significant departure of the surface-defined patterns is seen for either Bi or Te adlayers in the whole range of considered coverages because of the separation of the adatoms on the Pt(110) and (100).

3.3. Evolution of adsorption energy with coverage

The evolution of E_{ads} with the adatom coverage is summarized in Fig. 3. It is evident that addition of a new adatom gradually destabilizes the adlayers in agreement with experimentally observed trend for Bi adlayers on Pt(111) [51]. This trend is exactly opposite to that seen in systems where *d*-metals such as Pd, Pt, and Ni, are adsorbed on Pt [18,28], resulting in a strengthening of the adlayer-substrate interaction with each newly added adatom. This difference can be tied to the repulsive adatom-adatom interaction seen in the Bi(Te)/Pt systems, whereas attractive adatom-adatom interactions take place in adlayers of *d*-metals. Another factor contributing to the destabilization of the Bi and Te adlayers may be larger atomic radii of Bi and Te than that of the late *d*-metals such as Pd, Pt and Ni, suggesting that the atomic radius of the adatoms is an important factor driving the formation of the adlayer.

It must be noted that by comparing the adsorption energy of n^{th} adatom to corresponding bulk cohesion energy, E_{coh}, it can be concluded whether the new added adatom would adsorb on the available surface sites or it would rather interact with adatoms forming a three-dimensional structure [63–65]. The bulk cohesion energy values, calculated for stable rhombohedral crystal structure of Bi and the trigonal structure for Te, were −2.31 eV and −2.25 eV, resp. These values are somewhat more negative than the corresponding experimental ones of −2.18 eV and −2.19 eV [66]. Nonetheless, similar discrepancies between theoretical and experimental cohesion energy values were reported for transition metals [67].

Thus, using the calculated E_{coh} values, a formation of 3D structures for both Bi and Te would be predicted at coverages above 0.38 ML on Pt (111). However, planar adlayers for both species were found to be more stable than possible 3D structures, in agreement with the results obtained experimentally for Bi adlayers on Pt(111) where planar adlayers were formed at coverages below 0.56 ML [51]. In this regard, the thickness at which the properties of supported metallic adlayers start to resemble those of the pure metal surfaces depends on the nature of the metal [68]. Thus, it is possible that the coverages of Bi and Te, considered in the present study, are not enough to recreate their bulk properties, including the cohesion energy.

Also, as discussed above, the Bi and Te adlayers on Pt(111) experience a tensile strain, potentially further affecting their fundamental properties [69]. The combination of these factors can be the reason behind formation of the planar overlayers of Bi and Te on Pt(111) in the range of coverages up to half a monolayer even though adatom-surface interaction is weaker than cohesion energy of bismuth or tellurium.

Interestingly, tellurium is initially more stable than bismuth on all model surfaces, however, on Pt(111) Te adlayer becomes less stable than Bi adlayer after $\Theta = 0.31$ ML is reached where 5 adatoms are present on the surface. The same tendency is seen on Pt(100) closer to half a monolayer coverage, evidencing that after a certain $\Theta_{Bi(Te)}$ is reached on these surfaces, a noticeable change in Bi–Pt and Te–Pt interactions takes place.

A noteworthy feature is present for both adlayers on Pt(111) at 0.33 ML coverage, specifically, an approximately 0.5 eV stabilization is seen for Bi and Te. This stabilization arises mainly because on the $(2\sqrt{3} \times 2\sqrt{3})$ supercell the four Bi or Te adatoms are able to organize in a rhombus-like pattern with the average adatom-adatom distance close to 4.8 Å, more separated than at the 0.31 ML coverage, where this distance was 3.9 Å. Due to this separation the repulsive adatom-adatom interaction is lower at 0.33 ML coverage than at 0.31 ML coverage, resulting in the E_{ads} stabilization seen in Fig. 3. Interestingly, the rhombus-like pattern for the adlayers at $\Theta_{Bi(Te)} = 0.33$ ML is similar to that seen at 0.25 ML coverage, the main difference is that on the $(2\sqrt{3} \times 2\sqrt{3})$ supercell the 4 adatoms form a $(\sqrt{3} \times \sqrt{3})R30^o$ pattern sitting on the hcp sites separated from each other by an fcc site, rather than by the surface hcp site as they are at the 0.25 ML coverage (see Fig. 2). As the result the 4.8 Å of adatom-adatom distances at $\Theta_{Bi(Te)} = 0.33$ ML are significantly shorter than the 5.6 Å at $\Theta_{Bi(Te)} = 0.25$ ML, and the adlayer is less stable at higher coverage despite similar geometry.

For the adlayers on Pt(110), a significant destabilization is seen at $\Theta_{Bi(Te)} = 0.22$ ML, with the addition of 4th adatom to the system, as seen on Fig. 2 where rapid decrease appears for E_{ads}, while adsorption energies on Pt(111) and Pt (100) decrease mostly in a monotonous fashion. Regardless of the nature of the adsorbing species, a small plateau is seen on Pt(110), followed by a stabilization of the adlayer with 7 atoms. After this, the addition of 8th and 9th atoms leads to a gradual destabilization of the adlayers, despite both Bi and Te adsorbing on the same four-fold hollow site in the whole considered range of coverages.

This difference in adsorption energy trends on the considered platinum surfaces may be a result of the substrate geometry affecting the adlayer structure. It was demonstrated above that at lower coverages repulsive Te–Te interaction is stronger than the Bi–Bi one. Thus, on the most densely packed Pt(111) the tellurium adlayer destabilizes faster with the coverage than on Pt(100), where the repulsive adatom–adatom interactions are mitigated by higher separation of the adsorbed species on it. As the result on Pt(111) Bi adlayer becomes more stable than the Te overlayer at lower coverage compared to the Pt(100). At the same time, on the least densely packed Pt(110), the repulsive Te–Te interaction is nearly eliminated and tellurium remains more stable than bismuth in the whole range of the considered coverages.

Importantly, inclusion of spin–orbit coupling effects resulted in the same E_{ads} *vs.* $\Theta_{Bi(Te)}$ trends, introducing an almost constant shift of adsorption energies toward more negative values (Fig. S3). As it was discussed above, the non-SOC values for adsorption energies of bismuth in Bi/Pt(111) and Bi/Pt(100) are in better agreement with available experimental data. Thus, it can be argued that SOC is not strictly required for the analysis of adsorption energy changes with Bi and Te coverage.

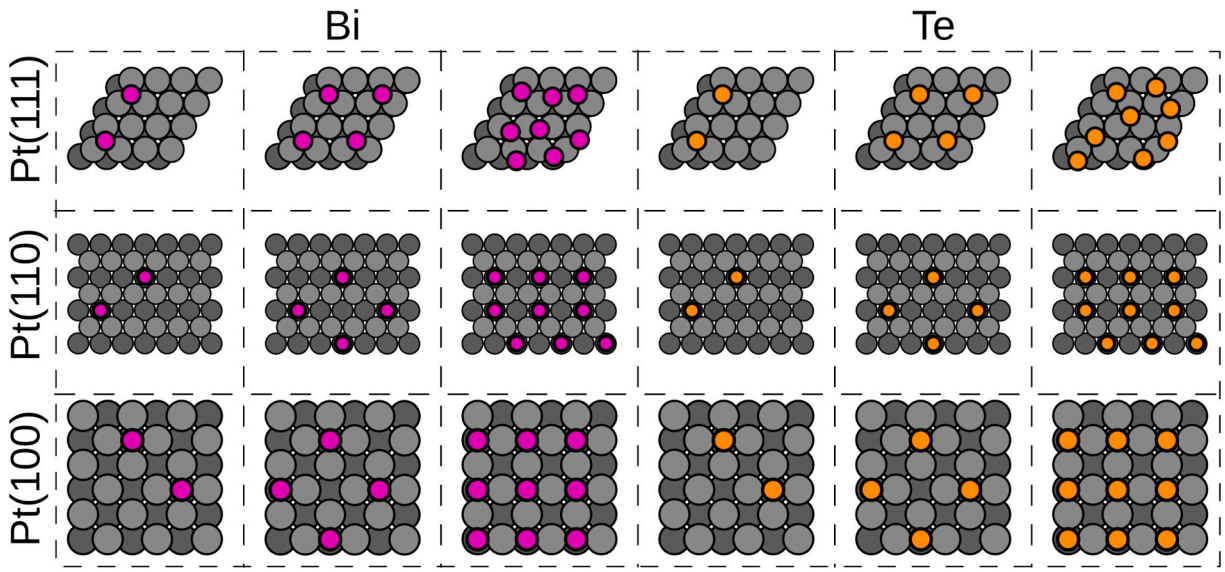

Fig. 2. Stable geometries for selected coverages of Bi and Te on Pt model surfaces. For Pt(111) coverages of 0.12 ML, 0.25 ML and 0.50 ML are illustrated; for Pt(110) and Pt(100) – coverages of 0.11 ML, 0.22 ML and 0.50 ML are shown. Light grey, dark grey, magenta and ochre spheres denote surface Pt, sublayer Pt, Bi and Te atoms, resp.

3.4. Changes on d-band centre upon adatom adsorption

The evolution of the electronic structure of platinum surface atoms with adatom coverage can be analysed based on changes on the position of the *d*-band centre of Pt atoms directly in contact with Bi and Te ($\varepsilon_{d,cont}$) and of the average *d*-band centre of all platinum atoms in the topmost layer of each surface ($\varepsilon_{d,surf}$), as it is summarized in Fig. 4.

As discussed above, the adsorption of even a single Bi or Te adatom impacts the electronic structure of the surface atoms in contact with the adsorbate through locally generated strain and interaction of *s* and *p* outer shell electrons of Bi and Te with 5*d* electrons of Pt [29]. A single Bi or Te adatom causes a downshift for both $\varepsilon_{d,cont}$ and $\varepsilon_{d,surf}$ toward more negative values, and this shift is larger in the Te/Pt systems, regardless of the geometry of the substrate. At this low coverage the total number of surface atoms interacting with the adsorbates is 3 out of 16 for Pt(111) and 4 out of 18 – for Pt(110) and Pt(100), thus, the change in $\varepsilon_{d,cont}$ is much higher compared to that in $\varepsilon_{d,surf}$.

With the increasing $\Theta_{Bi(Te)}$ more and more surface Pt atoms become involved into adsorbate–substrate interaction and the difference between $\varepsilon_{d,cont}$ and $\varepsilon_{d,surf}$ decreases. Starting with 0.33 ML coverage on Pt (111), all platinum atoms in the topmost layer interact with the adatoms and $\varepsilon_{d,cont}$ and $\varepsilon_{d,surf}$ converge. For Pt(110) this convergence takes place at $\Theta_{Bi(Te)} = 0.33$ ML, where 6 adatoms are present on the surface, and for Pt(100) – at $\Theta_{Bi(Te)} = 0.44$ ML, with 8 adatoms interacting with platinum. This difference arises from the specific geometry of each surface and the adatom coordination in each case.

The coverage $\Theta_{Bi(Te)}$ at which $\varepsilon_{d,cont}$ and $\varepsilon_{d,surf}$ converge on Pt(111) and Pt(100) is close the coverage where the Te adlayer becomes less stable than the Bi adlayer on these surfaces (Fig. 3). This correlation indicates that the change in adlayer stability with coverage can be linked to the number of surface Pt atoms affected by the presence of the adatoms. Because Te impact on the Pt ε_d is higher compared to that of Bi, the cumulative effect of Te on the electronic structure of platinum is greater once all surface atoms are involved into interaction with the overlayer, ultimately leading to a more pronounced destabilization of the Te overlayer.

Importantly, at lower coverages the electronic structure of the surface platinum atoms located sufficiently far from the adatoms is not affected. With growing coverage, however, the number of unaffected surface platinum atoms will decrease and, eventually, there will no

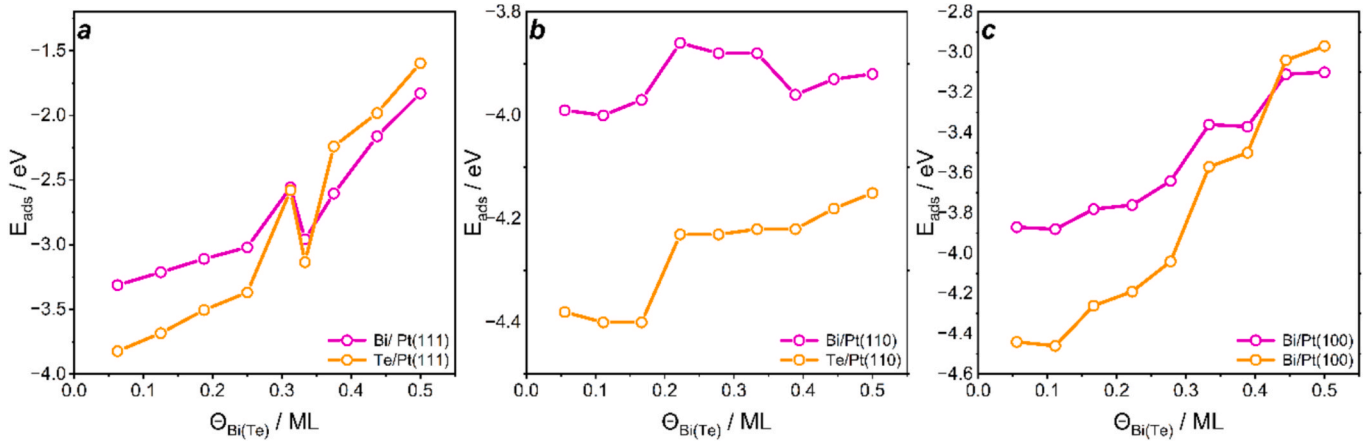

Fig. 3. Differential adsorption energies for Bi and Te on Pt model surfaces in the range of coverages from 0.06 ML to 0.50 ML for Pt(111) (panel *a*) and from 0.05 ML to 0.50 ML – for Pt(110) (panel *b*) and Pt(100) (panel *c*). Magenta and ochre dashed horizontal lines indicate cohesion energies of Bi and Te, respectively. Note that for Pt(100) and Pt(110) values of cohesive energies are outside of the y-axis scale.

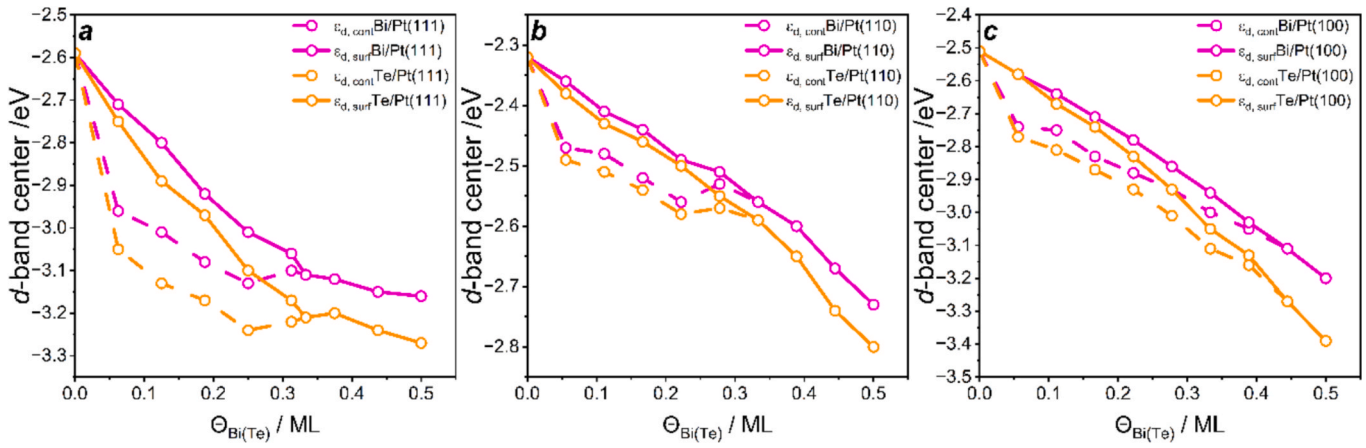

Fig. 4. Changes in the *d*-band centre position of Pt atoms in the Bi(Te)/Pt(111) (panel *a*), Bi(Te)/Pt(110) (panel *b*), and Bi(Te)/Pt(100) (panel *c*) systems. Average values for ε_d of Pt atoms in the topmost layer of each surface and atoms directly interacting with adatoms are indicated with solid and dashed lines, respectively.

unmodified Pt sites. Simultaneously, the properties of atoms in the Bi and Te adlayers will be different from those of pure bismuth or tellurium, due to the present charge transfer and strain. Thus, the systems comprising overlayers of Bi and Te supported on Pt cannot be treated as a mere combination of their parts and, instead, must be considered as unique materials with properties different from their parent systems.

3.5. Changes in the work function with adatom coverage

Calculated work functions for Pt(111), (110) and (100) were 5.79 eV, 5.50 eV, and 5.64 eV, respectively, being in a good agreement with experimental values of 5.91 eV, 5.53 eV, and 5.67 eV [70] and theoretical data obtained with the PBE functional [25,71].

As it can be appreciate from Fig. 5, an example of the unique properties of the Bi/Pt and Te/Pt systems compared to those of the parent materials is the induced change in the work function, $\Delta\Phi$, and it evolution with $\Theta_{Bi(Te)}$. In general, in absence of an external field, there are three main contributions to the change of the work function induced by adatoms [72,73]: the surface dipole density of the free-standing adsorbate layer, the charge rearrangement upon adsorption, and the substrate relaxation induced by the adsorbed layer. For the systems discussed here, an analysis of charge distribution and dipole change has been previously shown that the charge rearrangement upon adsorption is the most important factor in determining $\Delta\Phi$ at the lowest coverage [29].

Analogously, a similar analysis for higher coverages evidences that the sign and magnitude of $\Delta\Phi$ closely follows the sign and magnitude of the bond dipole associated with the modification of the electrostatic potential upon bond, as shown in Fig. S4.

Thus, charge rearrangement upon adsorption is the main reason of the change of the work function induced by adatoms, and the sign of $\Delta\Phi$ can be estimated from the direction of the charge transfer in the modified system. In this case, when the substrate is more electronegative than the adatom, the resulting negative dipole would be pointing toward the vacuum because of the"adatom → surface" charge transfer and the work function will decrease, i.e. $\Delta\Phi < 0$. In the opposite case, if the adsorbate is more electronegative than the substrate, the "adatom ← surface" charge transfer will take place, causing a negative charge build-up on the outside of the surface and positive charge accumulation within it. This would lead to a negative surface dipole, pointing toward the surface, causing the work function to increase, i.e. $\Delta\Phi > 0$.

Fig. 5 demonstrates that both Bi and Te lower the work function of the model platinum surface in the whole range of considered coverages. *I.e.* upon adsorption of either Bi or Te atom the work function decreases, regardless the orientation of the surface, being in agreement with positive charge build-up on the adatoms seen both from charge density difference [29] and either Mulliken, Hirshfield [5], Bader or DDEC6 partition schemes (see Table1). Thus, no additional analysis of changes in the surface dipole moments upon the adatom adsorption has been

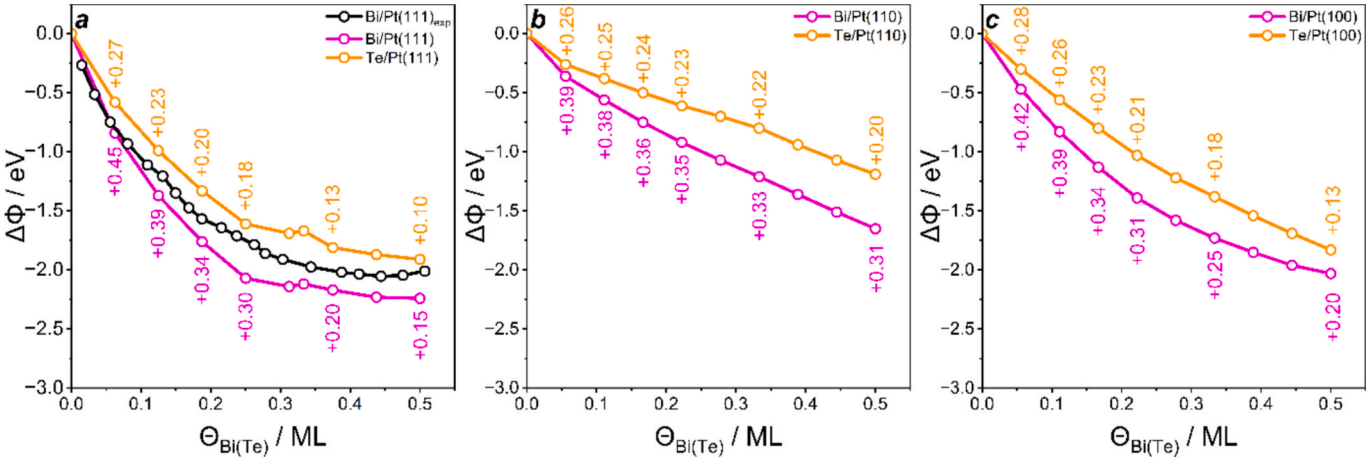

Fig. 5. Calculated changes in the work function for Pt model surfaces upon Bi and Te adsorption in the range of coverages from 0.06 ML to 0.50 ML for Pt(111) (panel a) and from 0.05 ML to 0.50 ML – for Pt(110) (panel b) and Pt(100) (panel c). Average values for partial charges are indicated for selected coverages. Experimental curve for the Bi/Pt(111) system was
adapted from [52].

performed here. It is noteworthy that while on bare surfaces Φ decreases in order (111) > (100) > (110), the presence of either of the adatom species lead to a new (100) > (110) > (111) trend, evidencing, thus, that the magnitude of the work function change strongly depends on the surface geometry. The observed adatom → surface charge transfer agrees well with an experimental study that attributed less favourable OH adsorption during oxygen reduction reaction to the charge transfer from Te to Pt and additional negative charge buildup on Pt [26].

The changes in Φ are larger for the Bi/Pt systems compared to those in Te/Pt surfaces with the same substrate geometry and these changes are in agreement with the difference in electronegativities of Pt and the adatoms, decreasing in order: $\xi_{Pt} > \xi_{Te} > \xi_{Bi}$ [74]. Importantly, inclusion of spin–orbit coupling effects changes the calculated work function values only marginally, by values not exceeding 0.04 eV, which is within the numerical accuracy of the method. Therefore, inclusion of SOC does not affect the conclusions drawn from calculations relying on scalar-relativistic approximation (non-SOC calculations). Similarly, as it was discussed above, accounting for SOC effect does not alter overall trends in adsorption energies for the studied systems. Thus, a conclusion can be made that including SOC effects is not required to capture adsorption trends in Bi/Pt and Te/Pt systems in the range of coverages considered in the present study.

There is no experimental data available on evolution of the work function of platinum surfaces with growing coverage of bismuth and tellurium, except for the Bi/Pt(111). For this system the calculated trend is on average 0.2 eV below the experimental values [51] (Fig. 5). These discrepancies may be due to differences in the theoretical and experimentally observed overlayer structures, which may arise because the approach, used in the present study, does not account for possible non-zero temperature adlayer disordering that is inevitably present in the experimental results obtained at 110 K and at ~ 600 K.

It can be seen that the geometry of the substrate has an impact on how the work function decreases with the adatom coverage. On the least densely packed Pt(110) surface the $\Delta\Phi$ *vs.* $\Theta_{Bi(Te)}$ trends are almost linear for both adsorbing species, while on more densely packed (100) surface a small curvature appears, especially evident for Bi, and the plot becomes slightly steeper. Finally, on the most densely packed Pt(111) the curves have the steepest descent between 0.06 ML and 0.25 ML, after which they reach a stable region where work function only decreases slightly with each added Bi or Te adatom. For this last surface, a similar feature has been observed in the work of Paffett, Campbell and Taylor [51], although the experimental curve passes through a small minimum close to $\Theta_{Bi} = 0.40$ ML and the stable region is located between 0.60 ML and 1.2 ML coverages.

Changes in the work function, $\Delta\Phi$ for a given surface are linearly connected to changes in the surface dipole, $\Delta\mu$, through the Helmholtz equation, $\Delta\mu = \frac{e}{\varepsilon_0}\frac{\Delta\Phi A}{\Theta}$, where A is the slab surface area, Θ – adatom coverage, e – elementary charge and ε_0 is vacuum permittivity. Therefore, presence of the stable region where the change in the work function with the increasing adatom coverage is minimal ($\Theta_{Bi(Te)} \approx 0.25$ ML – 0.50 ML) indicates that the net surface dipole per adatom undergoes only small changes in this range of coverages. This small change in $\Delta\mu$ could evidence depolarization of the adlayers, i.e. a reduction in the local dipole moment associated with each adatom as coverage increases. Specifically, the adatoms initially positive at lower coverages, become less positively charged because of charge redistribution within the adlayer and back-donation from the surface, resulting in the smaller contributions to the overall surface dipole.

The observed trend in the net adatom charges supports this interpretation. Both Bi and Te species become progressively less positively charged with the increasing coverage, this effect being the most noticeable on Pt(111), followed by Pt(100) and the smallest – on Pt (110). This trend can be directly linked to the adatom-adatom distances on these surfaces, which determines the degree of lateral repulsion and polarization within the adlayer. On Pt(111), the adatoms are closest to each other, forming a distorted pattern with the strongest lateral interactions. The depolarization of the adlayer reduces the repulsive dipole–dipole interaction, and adatoms are able to approach each other without significantly increasing the surface dipole.

A similar explanation has been proposed for alkali metals adsorbed on Pt [53], and for the Bi/Pt(111) system [51]. The rapid decrease in the work function up to a certain coverage followed by a slower decrease at higher coverages, without an obvious minimum, has been also reported for *sp*-metal adlayers on Pt(111) such as Sn [28]. Conversely, the work function of the same surface with adlayers of *d*-metals such as Ni, Pd, Pt, Cu, and Au, passes through a well-defined minimum [18,28].

In contrast, on Pt(110) and Pt(100) the adatom are organised in well-ordered surface-defined geometries characterised by larger adatom-adatom distances that reduce lateral interactions, so depolarization is less pronounced, resulting in the semi-linear region in the $\Delta\Phi$ *vs.* $\Theta_{Bi(Te)}$ trend.

Depolarization of the adlayers also explains the trend observed for the adsorption energies decreasing with the growing $\Theta_{Bi(Te)}$. At low coverages the adatoms are strongly polarized, thus, producing larger local dipoles and weaker adatom-substrate interactions. With the increasing coverage and the adlayer depolarization, the local dipole moment of each adatom decreases, weakening the adatom-substrate interaction and reducing E_{ads}. Simultaneously, the reduced dipole moments decrease lateral adatom-adatom repulsion, stabilizing adatom-adatom interaction within the adlayer and allowing formation of Bi and Te adlayers denser than at lower coverages. This mechanism is consistent with the semi-linear $\Delta\Phi$ *vs.* $\Theta_{Bi(Te)}$ trend and the weakening of substrate-adlayer interactions with coverage (Fig. S5). More information is available in Section S4 of the Supplementary Information.

Overall, the obtained results highlight the orientation of the surface and the balance between adatoms interacting within the adlayer and with the substrate as the key factors in adlayer formation. The orientation of platinum surface plane affects adatoms packing, their lateral interactions and the evolution of adatom-surface charge transfer with the coverage. As the result, the depolarization of the adlayers with the increasing coverages is also surface-sensitive. Specifically, reduction of the local dipole moment associated with each adatom due to charge redistribution in the adlayers and back-donation from the substrate plays a central role in controlling both the work function and the adsorption energies in the Bi(Te)/Pt systems resulting in depolarization of the overlayers and weakening of adsorbate–substrate interaction.

3.6. *Adatom-induced changes in fundamental properties of platinum in context of electrocatalysis*

Designing catalysis for a target (electro)chemical process historically has been based on a "trial and error" strategy. However, advances in surface science, computational chemistry, and a better understanding of reaction mechanisms for target processes, are gradually shifting the catalyst design toward a more informed and systematic approach. In this regard, the results presented above cannot be directly used to fully explain the effect of either Bi or Te on catalytic properties of the practical platinum-based catalytic systems. They, however, provide insight into fundamental-level impact of these adatoms on platinum surfaces that have hitherto been overlooked or underestimated in the context of catalytic properties of the overall complex Bi/Pt and Te/Pt systems.

Also, it is important to emphasize that the results presented here were obtained for model surfaces in vacuum and do not explicitly account for the factors that affect catalytic activity in electrochemical environments, such as solvent effects, electrode potential, interfacial electric fields, and specific adsorption of reaction intermediates. Consequently, the adatom-induced changes in the electronic or structural properties of platinum surfaces alone do not provide quantitative predictions of catalytic activity under operating electrochemical conditions. These changes, however, have a direct impact on the interaction of reactants or reaction intermediates with the catalyst surface. Thus,

the trends discussed in the present study remain relevant for understanding changes in the catalytic properties of platinum decorated with bismuth or tellurium.

The connection between the catalytic activity of a material and the stability of a reactant was established more than a century ago by Sabatier [75], who proposed that for an optimal catalytic reaction the interaction of the catalyst with the reactant should be neither too weak, nor too strong. Later a linear relationship between the activation energy and the enthalpy change of an elementary reaction, or the Brønsted-Evans-Polanyi (BEP) relation, was established [76,77]. Applying the BEP principle to reactions that involve reactant adsorption on the surface of a catalyst enabled more efficient catalyst screening by plotting catalytic activity of different materials against adsorption energy of species participating in the reaction. The resulting volcano-shaped curve has the optimal catalyst close to its apex, since it binds reagents and products neither too strongly, nor too weakly, satisfying the Sabatier's principle.

Importantly, because electrochemical reactions occur on the surface of the catalyst, the adsorption and desorption of reactants and reaction intermediates is largely defined by the fundamental properties of the surface atoms. For instance, the *d*-band centre theory [6] establishes a correlation between the adsorbate stability and *d*-band centre position, offering a useful first estimate of catalytic activity of a given material.

For the hydrogen evolution reaction (HER), a process essential for academic electrochemistry and for energy conversion and storage technologies, one of the first volcano curves was reported by Trasatti, who used the energy of hydride formation, since at that time no experimental or theoretical data was available on hydrogen adsorption energy [4]. In the same work, a clear link between the catalytic activity of a metallic catalyst toward the HER and its work function was also established, evidencing that atomic hydrogen stability directly depends on Φ. More specifically, the logarithm of the exchange current density is linearly related to the work function of the metal, regardless of the detailed nature of the mechanism involved as the rate-determining step [4]. While departure from this correlation may arise under specific electrochemical conditions, the work function remains a valuable preliminary criterion to assess the reactivity toward the HER.

In the context of the HER, both Bi and Te adatoms would be expected to destabilize atomic hydrogen on the model platinum surfaces. Indeed, the universally seen ε_d downshift will cause a downward shift of the antibonding states, formed upon hydrogen *s* and platinum *d* states, weakening the Pt–H bond as the result [78]. Since Pt is already at the apex of the HER volcano curve [79], this effect would shift it to the weak-binding shoulder of the curve, predicting a decrease of its catalytic activity toward HER. Similar conclusions can be made from the decrease in Φ [4], which would be also expected to destabilise hydrogen adsorption, potentially decreasing catalytic activity of the composite Bi (Te)/Pt systems.

The impact of both adatom species on the fundamental properties of Pt is proportional to their coverage, as discussed above, thus, at very low $\Theta_{Bi(Te)}$ the decrease in the HER activity would be minimal. At sufficiently high coverages, however, all surface atoms would be affected and the deleterious effect of Bi and Te presence on the activity would become more evident.

To the knowledge of the authors there are no studies available on HER activity of the Te-modified platinum, however, the combined effect of the factors, discussed above, may contribute to the experimentally observed significant decrease in HER activity of platinum surfaces upon irreversible adsorption of Bi on them [12,13]. Interestingly, while adsorbed Bi has deleterious effect on the HER activity of platinum, a combined theoretical–experimental study showed that the HER activity of BiPt surface alloys is better than that of pure Pt because of their optimized hydrogen binding [80]. Despite their shortcoming as HER catalysts, practical Bi-adatom modified platinum surfaces show a greater promise for the electrooxidation of organic molecules such as formic acid [8,11,14,21,22], alcohols [15,16,23] and glucose [9,17,24]. In many of these studies the adatom-induced improvement in catalytic properties of platinum has been explained in the terms of the third-body effect, when the foreign atom blocks surface sites and steers reaction along a more optimal path.

Often, however, third-body effects alone are not enough to account for all observed activity changes. In this regard, it has been proposed that the adatom-modified Pt(111) catalytic activity toward formic acid oxidation (FAO) depends on whether the adatom species display a work function lower than platinum [20] and the bigger the difference between the work function of the modifying element and that of Pt, the more evident is the promoting effect. Based on this argument the catalytic activity of Bi/Pt systems ($\Phi_{Bi} = 4.22$ eV) would be higher than that of Te/Pt ($\Phi_{Te} = 4.95$ eV), which has been demonstrated experimentally in the same study.

Furthermore, the increase in the catalytic activity of platinum has been directly tied to the partial positive charge of the modifying atoms [5], since the presence of positively charged adatom promotes formic acid physisorption in a C–H down configuration, facilitating the C–H bond cleavage [81]. However, increasing the number of positively charged atoms on the surface would not necessarily lead to a proportionally increased catalytic activity of Pt toward FAO, because of positive charge on the adatoms decreases with their coverage, as discussed above.

In this regard, experimental studies of catalytic properties of Bi/Pt systems toward FAO evidenced that the maximum catalytic rate is achieved at the intermediate Bi coverages [19,82]. At these coverages the electronic properties of most of the surface Pt atoms are modified by presence of Bi adatoms and at the same time they remain available for interaction with the reaction intermediates. Conversely, it was proposed that at higher Bi coverages the adlayers are too populated to produce Bi-free Pt sites, resulting in the decreased catalytic performance toward FAO.

Similarly, enhanced catalytic activity of Pt, modified by a bismuth adlayer, toward the electrooxidation of alcohols is typically attributed to the third-body effect. However, it has been demonstrated that bismuth reduces the poisoning effect of strongly adsorbed species, such as CO, generated during ethanol electrooxidation [15]. Thus, the promoting effect of bismuth on catalytic activity of Pt in this case may also originate from the adatom-induced changes in the electronic properties of platinum surfaces, with the *d*-band centre downshift being a contributing factor to the improvement of catalytic properties of the overall system.

This effect is clearly coverage-sensitive, since the biggest enhancement of the activity toward ethanol oxidation has been observed for the system with relatively low $\Theta_{Bi} = 0.34$ ML [15]. At this coverage the adatoms affect electronic structure of all surface atoms, while leaving Pt-sites available for interaction with possible adsorbates resembling the optimal Bi coverages for FAO, discussed above.

The enhanced catalytic activity of Pt modified by adlayer of bismuth toward glucose electrooxidation is another example of the adatoms impact on the electrocatalitic activity of the substrate. Although in this case, a mechanism different from the third-body effect has been proposed. It has been remarked that Bi adsorbed on platinum, tends to bind OH^- from the alkaline solution, consequently sharing it with the neighbouring Pt [9], increasing the number of the main active species for electrooxidation of glucose on Pt. Another reason behind this improved activity could be an effect similar to that proposed in the Bi-modified Pd system [3], where the presence of bismuth facilitated the desorption of gluconate from the surface that reduces its poisoning by the reaction product, giving the significant decrease on the *d*-band centre reported above for Bi/Pt systems. In either case, adatoms affect the catalytic activity of the overall system through the bifunctional mechanism, which would directly depend on the adatom coverage.

Unfortunately, most of the experimental data available in the literature only concern Bi/Pt systems, leaving Te/Pt systems without much experimental comparison. Nonetheless, there is experimental evidence that the charge transfer from Te to platinum, and adatom-induced

downshift of platinum *d*-band centre destabilize OH adsorption on the Pt, which is consistent with the experimentally observed enhanced electrocatalysis for oxygen reduction reaction [26].

Also, undeniable similarities in the effects of Bi and Te would allow to extend the conclusions made for Bi-modified systems to those with Te adatoms. It can be seen that in practice it is extremely difficult to identify the mechanism by which adatoms affect catalytic properties of the host surface. Therefore, while developing novel catalytic materials, a detailed theoretical characterization could improve the understanding of the mechanism behind adatom impact on catalytic properties of complex substrate – adlayer systems toward a target reaction.

Although theoretical modelling of systems with higher adatom coverage is often demanding in terms of computational resources and time, accounting for the coverage effect is essential for the comprehensive description of substrate – adlayer systems in the context of their application in (electro)catalysis. In this regard, the present study offers an insight into the effect of multiple adatoms adsorbed on model platinum surfaces on their fundamental properties and contributes to the field of informed and systematic design of Pt-based catalysts.

4. Conclusions

A theoretical study has been conducted on the interaction of bismuth and tellurium with Pt(111), Pt(110) and Pt(100) surfaces in the range of the adatom coverage from 0.06 ML on Pt(111) and 0.05 ML – on the rest of the studied surfaces, up to half a monolayer. A systematic analysis of adsorption energies, geometries, and the adatom-induced evolution of important electronic properties of platinum surfaces provides insights into Bi–Pt and Te–Pt interactions on the atomistic level.

Good agreement was found between obtained results and literature data for a more studied Bi/Pt(111) system. Overall, both Bi and Te demonstrate a lot of similarities in their interaction with model platinum substrates. Even at the lowest considered coverages both Bi and Te noticeably affect Pt substrates, ceding charge to them, decreasing the work function, and shifting the *d*-band centre position of surface atoms interacting with the adatoms further away from the Fermi level.

At lower coverages adsorbed atoms of the same species interact repulsively with each other, thus, preferably occupying surface sites, at a distance from each other. At the coverages close to half a monolayer the decrease on the *d*-band centre of Pt atoms in contact to the adatom weakens the metal-adatom bond, while stabilizing the adatom-adatom interaction within the adlayer due to depolarization of the adatoms. Because of this while the addition of each new atom to the model surfaces gradually destabilizes the whole system (i.e. makes adsorption energies less negative) adlayers remain stable in the whole range of considered coverages. On more open Pt(110) and (100) surfaces the substrate-defined adlayer patterns remain in the whole range of coverages. Conversely, on densely packed Pt(111) the initially hexagonal pattern seen at lower coverages breaks with $\Theta_{Bi(Te)}$ approaching half a monolayer. In all cases the adlayers maintain planar geometry rather than forming 3D structures.

The tendencies observed for the impact of a single adatom on the work function of the surfaces and position of the *d*-band centre are retained at higher coverages. Specifically, lowering of the work function has been observed for all substrates, except for Pt(111). There, after the coverage of 0.25 ML was reached, further addition of Bi and Te adatoms causes only a slight decrease in Φ. This may indicate back donation of the charge from substrate to adlayers, which is in line with net positive charges on Bi and Te decreasing with coverage.

Regarding the *d*-band centre of the surface atoms in contact with the adatoms, a gradual decrease with the growing adlayers coverage is calculated. However, at coverages of 0.33 ML on Pt(111) and Pt(110) and 0.44 ML — on Pt(100), all platinum atoms in the topmost layer are in contact with adatoms, thus their impact on the electronic structure of the substrate becomes surface-wide. Combined with observed changes in the work function and charge distribution, adatom adsorption may entail a shift in catalytic properties of the whole composite Bi/Pt and Te/Pt systems toward important processes such as hydrogen evolution reaction and electrooxidation of formic acid, glucose and alcohols.

The obtained results offer valuable insights for a systematic understanding of the Pt-based catalysts, contributing to a better understanding of adlayer-substrate metallic systems in general. Conclusions drawn in present work can be potentially useful for a more informed and methodical approach to catalysts design and fine tuning of their properties.

CRediT authorship contribution statement

Andrey A. Koverga: Writing – original draft, Methodology, Investigation, Conceptualization. **Ana María Gómez-Marín:** Writing – review & editing, Validation, Methodology, Investigation, Conceptualization. **Elizabeth Flórez:** Writing – review & editing, Validation, Methodology. **Edson A. Ticianelli:** Writing – review & editing, Supervision, Validation, Methodology, Project administration.

Declaration of competing interest

The authors declare the following financial interests/personal relationships which may be considered as potential competing interests: Andrey A. Koverga reports financial support was provided by State of Sao Paulo Research Foundation. If there are other authors, they declare that they have no known competing financial interests or personal relationships that could have appeared to influence the work reported in this paper.

Acknowledgments

The authors would like to thank Fundação de Amparo a Pesquisa do Estado de São Paulo (FAPESP – Procs. 2020/11947-2 and 2019/22183-6), Brazil, for financial support and the Center for Mathematical Sciences Applied to Industrial (CeMEAI) for providing the computational resources for the research. Authors also express their gratitude to Universidad de Medellin

Appendix A. Supplementary material

Supplementary data to this article can be found online at https://doi.org/10.1016/j.apsusc.2026.166710.

Data availability

Data will be made available on request.

References

[1] R.R. Adžić, Electrocatalysis on surfaces modified by foreign metal adatoms, Isr. J. Chem. 18 (1979) 166–181.
[2] M. Watanabe, M. Horiuchi, S. Motoo, Electrocatalysis by ad-atoms, J. Electroanal. Chem. 250 (1988) 117–125.
[3] M. Wenkin, P. Ruiz, B. Delmon, M. Devillers, The role of bismuth as promoter in Pd–Bi catalysts for the selective oxidation of glucose to gluconate, J. Mol. Catal. A Chem. 180 (2002) 141–159.
[4] S. Trasatti, Work function, electronegativity, and electrochemical behaviour of metals, J. Electroanal. Chem. 39 (1972) 163–184.
[5] A. Ferre-Vilaplana, J.V. Perales-Rondón, J.M. Feliu, E. Herrero, Understanding the effect of the adatoms in the formic acid oxidation mechanism on Pt(111) electrodes, ACS Catal. 5 (2014) 645–654.
[6] A. Ruban, B. Hammer, P. Stoltze, H. Skriver, J. Nørskov, Surface electronic structure and reactivity of transition and noble metals, J. Mol. Catal. A Chem. 115 (1997) 421–429.
[7] J. Ontaneda, R.A. Bennett, R. Grau-Crespo, Electronic structure of Pd multilayers on Re(0001): the role of charge transfer, J. Phys. Chem. C 119 (2015) 23436–23444.
[8] S.A. Campbell, R. Parsons, Effect of Bi and Sn adatoms on formic acid and methanol oxidation at well defined platinum surfaces, J. Chem. Soc. Faraday Trans. 88 (1992) 833–841.

[9] Z. Yang, Y. Miao, L. Xu, G. Song, S. Zhou, Adsorption of Bi(III) on Pt nanoparticles leading to the enhanced electrocatalysis of glucose oxidation, Colloid J. 77 (2015) 382–389.
[10] A.M. Gomez-Marín, V. Briega-Martos, J.M. Feliu, Oxygen reduction on Te-modified Pt(111) surfaces: site-blocking vs electronic effects, J. Chem. Phys. 152 (2020) 164702.
[11] J. Clavilier, A. Fernandez-Vega, J. Feliu, A. Aldaz, Heterogeneous electrocatalysis on well defined platinum surfaces modified by controlled amounts of irreversibly adsorbed adatoms, J. Electroanal. Chem. 258 (1989) 89–100.
[12] R. Gomez, A. Fernandez-Vega, J.M. Feliu, A. Aldaz, Hydrogen evolution on platinum single crystal surfaces: effects of irreversibly adsorbed bismuth and antimony on hydrogen adsorption and evolution on platinum (100), J. Phys. Chem. 97 (1993) 4769–4776.
[13] R. Gomez, J.M. Feliu, A. Aldaz, Effects of irreversibly adsorbed bismuth on hydrogen adsorption and evolution on Pt(111), Electrochim. Acta 42 (1997) 1675–1683.
[14] S.P.E. Smith, K.F. Ben-Dor, H.D. Abruña, Poison formation upon the dissociative adsorption of formic acid on bismuth-modified stepped platinum electrodes, Langmuir 16 (1999) 787–794.
[15] R.G. Freitas, E.C. Batista, M.P. Castro, R.T.S. Oliveira, M.C. Santos, E.C. Pereira, Ethanol electrooxidation on Bi submonolayers deposited on a Pt electrode, Electrocatalysis 2 (2011) 224–230.
[16] I. Mahesh, R. Jaithaliya, A. Sarkar, Efficient electrooxidation of ethanol on Bi@Pt/C nanoparticles: (i) effect of monolayer Bi deposition on specific sites of Pt nanoparticle; (ii) Calculation of average number of e-s without help of chemical analysis, Electrochim. Acta 258 (2017) 933–941.
[17] P. Kanninen, T. Kallio, Activation of commercial Pt/C catalyst toward glucose electro-oxidation by irreversible Bi adsorption, J. Energy Chem. 27 (2018) 1446–1452.
[18] A.A. Koverga, A.M. Gomez-Marín, E. Flórez, Not a mere decoration: impact of submonolayer coverages of nickel on fundamental properties of platinum, J. Phys. Chem. C 126 (2022) 10167–10180.
[19] J.V. Perales-Rondón, A. Ferre-Vilaplana, J.M. Feliu, E. Herrero, Oxidation mechanism of formic acid on the bismuth adatom-modified Pt(111) surface, J. Am. Chem. Soc. 136 (2014) 13110–13113.
[20] E. Herrero, M. Llorca, J. Feliu, A. Aldaz, Oxidation of formic acid on Pt(111) electrodes modified by irreversibly adsorbed tellurium, J. Electroanal. Chem. 394 (1995) 161–167.
[21] S.P. Smith, H.D. Abruña, Structural effects on the oxidation of HCOOH by bismuth modified Pt(111) electrodes with (110) monatomic steps, J. Electroanal. Chem. 467 (1999) 43–49.
[22] D. Volpe, E. Casado-Rivera, L. Alden, C. Lind, K. Hagerdon, C. Downie, C. Korzeniewski, F.J. DiSalvo, H.D. Abruña, Surface treatment effects on the electrocatalytic activity and characterization of intermetallic phases, J. Electrochem. Soc. 151 (2004) A971–A979.
[23] M. Figueiredo, R. Arán-Ais, J. Feliu, K. Kontturi, T. Kallio, Pt catalysts modified with Bi: enhancement of the catalytic activity for alcohol oxidation in alkaline media, J. Catal. 312 (2014) 78–86.
[24] G. Wittstock, A. Strubing, R. Szargan, G. Werner, Glucose oxidation at bismuth-modified platinum electrodes, J. Electroanal. Chem. 444 (1998) 61–73.
[25] F. Gossenberger, T. Roman, K. Forster-Tonigold, A. Groß, Change of the work function of platinum electrodes induced by halide adsorption, Beilstein J. Nanotechnol. 5 (2014) 152–161.
[26] T.-T. Mao, Z. Wei, B.-Y. Liu, Y.-J. Xu, J. Cai, Y.-X. Chen, J.M. Feliu, E. Herrero, Electrocatalysis of oxygen reduction on Te-modified platinum stepped crystal surfaces, ACS Catal. 13 (2023) 16045–16054.
[27] I.A. Pašti, S.V. Mentus, Modification of electronic properties of Pt(111) surface by means of alloyed and adsorbed metals: DFT study, Russ. J. Phys. Chem. A 83 (2009) 1531–1536.
[28] I. Pašti, S. Mentus, First principles study of adsorption of metals on Pt(111) surface, J. Alloys Compd. 497 (2010) 38–45.
[29] A. Koverga, E. Flórez, M.A. Gomez–Marín, Electronic changes at the platinum interface induced by bismuth and tellurium adatom adsorption, Appl. Surf. Sci. 608 (2022) 155137.
[30] S. Schnur, A. Groß, Properties of metal–water interfaces studied from first principles, New J. Phys. 11 (2009) 125003.
[31] B.E. Hayden, A.J. Murray, R. Parsons, D.J. Pegg, UHV and electrochemical transfer studies on Pt(110)-(1x2): the influence of bismuth on hydrogen and oxygen adsorption, and the electro-oxidation of carbon monoxide, J. Electroanal. Chem. Interfacial Electrochem. 409 (1996) 51–63.
[32] U.W. Hamm, D. Kramer, R.S. Zhai, D.M. Kolb, On the valence state of bismuth adsorbed on a Pt(111) electrode—An electrochemistry, LEED and XPS study, Electrochim. Acta 43 (1998) 2969–2978.
[33] T.J. Schmidt, B.N. Grgur, R.J. Behm, N.M. Markovic, P.N. Ross, Bi adsorption on Pt (111) in perchloric acid solution : a rotating ring-disk electrode and XPS study, Phys. Chem. Chem. Phys. 2 (2000) 4379–4386.
[34] T.J. Schmidt, V.R. Stamenkovic, C.A. Lucas, N.M. Markovic, P.N. Ross Jr., Surface processes and electrocatalysis on the Pt(hkl)/Bi-solution interface, Phys. Chem. Chem. Phys. 3 (2001) 3879–3890.
[35] C.K. Rhee, D.-K. Kim, Electrochemical scanning tunneling microscope study of irreversibly adsorbed Te on a Pt(111) single crystal electrode surface, J. Electroanal. Chem. 506 (2001) 149.
[36] W. Zhou, L. Kibler, D. Kolb, Evidence for a change in valence state for tellurium adsorbed on a Pt(111) electrode, Electrochim. Acta 47 (2002) 4501–4510.
[37] G. Kresse, J. Hafner, Ab initio molecular dynamics for liquid metals, Phys. Rev. B 47 (1993) 558–561.
[38] G. Kresse, J. Hafner, Ab initio molecular dynamics simulation of the liquid metal amorphous semiconductor transition in germanium, Phys. Rev. B 49 (1994) 14251–14269.
[39] G. Kresse, J. Furthmuller, Efficient iterative schemes for ab initio total-energy calculations using a plane-wave basis set, Phys. Rev. B 54 (1996) 11169–11186.
[40] G. Kresse, J. Furthmuller, Efficiency of ab-initio total energy calculations for metals and semiconductors using a plane-wave basis set, Comput. Mater. Sci 6 (1996) 15–50.
[41] J.P. Perdew, K. Burke, M. Ernzerhof, Generalized gradient approximation made simple, Phys. Rev. Lett. 77 (1996) 3865–3868.
[42] M.J. Ungerer, D. Santos-Carballal, A. Cadi-Essadek, C.G.C.E. van Sittert, N.H. de Leeuw, Interaction of H2O with the platinum Pt(001), (011), and (111) surfaces: a density functional theory study with long-range dispersion corrections, J. Phys. Chem. C 123 (2019) 27465–27476.
[43] K. Okuda, M. Alaydrus, N. Hoshi, I. Hamada, M. Nakamura, Electrical double layer on the Pt(111) electrode modeled under ultrahigh vacuum conditions, J. Phys. Chem. C 126 (2022) 4726–4732.
[44] A.A. Koverga, E. Flórez, J.A. Rodriguez, Pushing Cu uphill of the volcano curve: impact of a WC support on the catalytic activity of copper toward the hydrogen evolution reaction, Int. J. Hydrogen Energy 46 (2021) 25092–25102.
[45] P.E. Blöchl, Projector augmented-wave method, Phys. Rev. B 50 (1994) 17953–17979.
[46] G. Kresse, D. Joubert, From ultrasoft pseudopotentials to the projector augmented-wave method, Phys. Rev. B 59 (1999) 1758–1775.
[47] H.J. Monkhorst, J.D. Pack, Special points for Brillouin-zone integrations, Phys. Rev. B 13 (1976) 5188–5192.
[48] M. Methfessel, A.T. Paxton, High-precision sampling for Brillouin-zone integration in metals, Phys. Rev. B 40 (1989) 3616–3621.
[49] J.L.D. Silva, C. Stampfl, M. Scheffler, Converged properties of clean metal surfaces by all-electron first-principles calculations, Surf. Sci. 600 (2006) 703–715.
[50] K. Krupski, M. Moors, P. Jóźwik, T. Kobiela, A. Krupski, Structure determination of Au on Pt(111) surface: LEED STM and DFT study, Materials 8 (2015) 2935–2952.
[51] M.T. Paffett, C.T. Campbell, T.N. Taylor, Adsorption and growth modes of Bi on Pt (111), J. Chem. Phys. 85 (1986) 6176–6185.
[52] N. Kizhakevariam, E.M. Stuve, Coadsorption of bismuth with electrocatalytic molecules: a study of formic acid oxidation on Pt(100), J. Vac. Sci. Technol. A 8 (1990) 2557–2562.
[53] H. Bonzel, Alkali-metal-affected adsorption of molecules on metal surfaces, Surf. Sci. Rep. 8 (1988) 43–125.
[54] A.A. Koverga, E. Flórez, C. Jimenez-Orozco, J.A. Rodriguez, Not all platinum surfaces are the same: effect of the support on fundamental properties of platinum adlayer and its implications for the activity toward hydrogen evolution reaction, Electrochim. Acta 368 (2021) 137598.
[55] T.A. Manz, D.S. Sholl, Improved atoms-in-molecule charge partitioning functional for simultaneously reproducing the electrostatic potential and chemical states in periodic and nonperiodic materials, J. Chem. Theory Comput. 8 (2012) 2844–2867.
[56] T.A. Manz, N.G. Limas, Introducing DDEC6 atomic population analysis: part 1 charge partitioning theory and methodology, RSC Adv. 6 (2016) 47771–47801.
[57] R.F.W. Bader, Atoms in Molecules: A Quantum Theory, Oxford University Press, Oxford, 1990.
[58] G. Henkelman, A. Arnaldsson, H. Jonsson, A fast and robust algorithm for Bader decomposition of charge density, Comput. Mater. Sci 36 (2006) 354–360.
[59] A. Vojvodic, J.K. Nørskov, F. Abild-Pedersen, Electronic structure effects in transition metal surface chemistry, Top. Catal. 57 (2013) 25–32.
[60] A.A. Koverga, E.A. Ticianelli, A. Groß, Interaction of Li, Na and K overlayers with Pt(111): Structure and fundamental properties, Appl. Surf. Sci. 718 (2026) 164918.
[61] A. Michaelides, P. Hu, M.-H. Lee, A. Alavi, D.A. King, Resolution of an ancient surface science anomaly: work function change induced by N adsorption on W {100}, Phys. Rev. Lett. 90 (2003) 246103.
[62] T.A. Maark, A.A. Peterson, Understanding strain and ligand effects in hydrogen evolution over Pd(111) surfaces, J. Phys. Chem. C 118 (2014) 4275–4281.
[63] C.B. Krishnamurthy, O. Lori, L. Elbaz, I. Grinberg, First-principles investigation of the formation of Pt nanorafts on a Mo_2C support and their catalytic activity for oxygen reduction reaction, J. Phys. Chem. Lett. 9 (2018) 2229–2234.
[64] D.V. Esposito, S.T. Hunt, Y.C. Kimmel, J.G. Chen, A new class of electrocatalysts for hydrogen production from water electrolysis: metal monolayers supported on low-cost transition metal carbides, J. Am. Chem. Soc. 134 (2012) 3025–3033.
[65] S. Wannakao, N. Artrith, J. Limtrakul, A.M. Kolpak, Engineering transition-metal-coated tungsten carbides for efficient and selective electrochemical reduction of CO_2 to methane, ChemSusChem 8 (2015) 2745–2751.
[66] C. Kittel, Introduction to Solid State Physics, John Wiley & Sons, New York, 1986.
[67] P. Janthon, S.A. Luo, S.M. Kozlov, F. Viñes, J. Limtrakul, D.G. Truhlar, F. Illas, Bulk properties of transition metals: a challenge for the design of universal density functionals, J. Chem. Theory Comput. 10 (2014) 3832–3839.
[68] S. Trasatti, in: Comprehensive Treatise of Electrochemistry, Springer, US, 1980, pp. 45–81.
[69] X. Zheng, L. Li, J. Li, Z. Wei, Intrinsic effects of strain on low-index surfaces of platinum: roles of the five 5d orbitals, Phys. Chem. Chem. Phys. 21 (2019) 3242–3249.
[70] M. Salmeron, S. Ferrer, M. Jazzar, G.A. Somorjai, Photoelectron-spectroscopy study of the electronic structure of Au and Ag overlayers on Pt(100), Pt(111), and Pt (997) surfaces, Phys. Rev. B 28 (1983) 6758–6765.
[71] N.E. Singh-Miller, N. Marzari, Surface energies, work functions, and surface relaxations of low-index metallic surfaces from first principles, Phys. Rev. B 80 (2009) 235407.

[72] T.C. Leung, C.L. Kao, W.S. Su, Y.J. Feng, C.T. Chan, Relationship between surface dipole, work function and charge transfer: some exceptions to an established rule, Phys. Rev. B 68 (2003) 195408.
[73] P.S. Bagus, D. Käfer, G. Witte, C. Wöll, Work function changes induced by charged adsorbates: origin of the polarity asymmetry, Phys. Rev. Lett. 100 (2008) 126101.
[74] A.L. Allred, Electronegativity values from thermochemical data, J. Inorg. Nucl. Chem. 17 (1961) 215–221.
[75] P. Sabatier, La Catalyse en Chimie Organique, Librairie polytechnique, Paris et Liege, 1920.
[76] J.N. Bronsted, Acid and basic catalysis, Chem. Rev. 5 (1928) 231–338.
[77] M.G. Evans, M. Polanyi, Inertia and driving force of chemical reactions, Trans. Faraday Soc. 34 (1938) 11–24.
[78] B. Hammer, J. Nørskov, Electronic factors determining the reactivity of metal surfaces, Surf. Sci. 343 (1995) 211–220.
[79] J.K. Nørskov, T. Bligaard, A. Logadottir, J.R. Kitchin, J.G. Chen, S. Pandelov, U. Stimming, Trends in the exchange current for hydrogen evolution, J. Electrochem. Soc. 152 (2005) J23–J26.
[80] J. Greeley, T.F. Jaramillo, J. Bonde, I. Chorkendorff, J.K. Nørskov, Computational high-throughput screening of electrocatalytic materials for hydrogen evolution, Nat. Mater. 5 (2006) 909–913.
[81] B. Peng, H.-F. Wang, Z.-P. Liu, W.-B. Cai, Combined surface-enhanced infrared spectroscopy and first-principles study on electro-oxidation of formic acid at Sb-modified Pt electrodes, J. Phys. Chem. C 114 (2010) 3102–3107.
[82] H. Lee, Y.J. Kim, Y. Sohn, C.K. Rhee, The ways for Bi on Pt to enhance formic acid oxidation, J. Electrochem. Sci. Technol. 14 (2023) 21–30.